ISSN 2831-1434

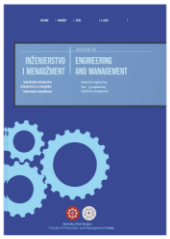

Journal homepage: https://jem.fpm.ues.rs.ba/index.php/journal

Journal of Engineering and Management

Volume 3 / No 2 / October 2025 / 35-45

UDK 517.91:[621.1:536.2

DOI 10.7251/JEM2502035G

COBISS.RS-ID 143667201

Original Research Paper

Full Discrete Forms of Heat Conduction Equation by Meshless Fragile Points Method (FPM) and Various ODE Solvers

Potpuno diskretizovane formulacije jednačine toplotne provodljivosti na bazi bezmrežne *Fragile Points* metode (FPM) i različitih algoritama za rješavanje ODJ

R. Grujičić

University of Montenegro, Faculty of Mechanical Engineering, Dzordza Vasingtona bb 81000 Podgorica, Montenegro

Abstract: *According to recent studies, the Fragile Points Method (FPM) has emerged as a highly promising technique for addressing problems related to heat conduction analysis. This paper further develops and extends the investigation of FPM by implementing and comparing several explicit and implicit time integration schemes for solving the resulting systems of ordinary differential equations (ODEs). In total, six fully discrete formulations of the general heat conduction equation are derived and presented. The study includes a detailed assessment of each algorithm's computational complexity, execution time, and relative numerical accuracy, providing a comprehensive evaluation of their performance. The convergence and stability of the FPM approach were verified through multiple benchmark problems with known analytical solutions in both one and two dimensions. Furthermore, it was demonstrated that the presence of non-homogeneity and anisotropy in the analysed media does not introduce additional difficulties for the method. When compared with explicit techniques, the implicit formulations proved to be more efficient for stiff problems, achieving stable solutions while maintaining comparable computational costs.*

Key words: *Fragile Points Method, Heat Conduction Equation, Ordinary Differential Equation*

Apstrakt: *Skorija istraživanja su pokazala da se Fragile Points metoda (FPM) pokazala kao veoma perspektivna tehnika za rješavanje problema koji se odnose na analizu provođenja toplote. Ovaj rad za cilj ima dalji razvoj i širenje istraživanja u pravcu primjene FPM za konkretan problem uvođenjem i međusobnim poređenjem nekoliko eksplicitnih i implicitnih šema za vremensku integraciju kako bi se riješio rezultujući sistem običnih diferencijalnih jednačina (ODJ). Ukupno je razvijeno i predstavljeno šest potpuno diskretizovanih formi opšte jednačine provođenja toplote. Istraživanje obuhvata detaljnu procjenu računske efikasnosti, vremena izvršenja koda i relativne numeričke preciznosti za svaki od algoritama, pružajući sveobuhvatnu procjenu njihovih karakteristika. Konvergentnost i stabilnost pristupa na bazi FPM su verifikovani rješavanjem nekoliko problema sa poznatim analitičkim rješenjima u jednoj i dvije dimenzije. Pored toga, pokazano je da prisustvo nehomogenosti i anizotropnosti analiziranih sredina ne predstavlja nikakvu prepreku za posmatranu metodu. U poređenju sa eksplicitnim tehnikama, implicitne metode su se pokazale kao efikasnije za tzv. krute (stiff) probleme, dajući stabilne rezultate uz očuvanje niskih računskih troškova.*

Ključne riječi*: Fragile Points metoda, jednačina provođenja toplote, obična diferencijalna jednačina*

1 INTRODUCTION

Although many physical processes are well described by partial differential equations (PDEs), analytical solutions are unavailable for most of them. Moreover, analytical results are often restricted to simplified models that do not always accurately represent the real behaviour of the system. To address these limitations, numerous numerical methods for solving PDEs and

radeg@ucg.ac.me

performing simulations have been developed over the past several decades.

One of the more recent approaches is the Fragile Points Method (FPM), introduced by Dong et al. [1]. While retaining the essential advantages over the classical mesh-based methods, it also offers computational improvements compared to other meshless approaches. Its main feature lies in the use of discontinuous polynomial trial functions, which allow for easy, precise, and efficient integration using simple Gaussian quadratures.

So far, the FPM has shown great potential for solving various types of problems, including heat conduction problems, as reported in several studies [2–6].

This paper extends previous research by focusing on the compatibility of FPM with various explicit and implicit solvers, as well as on the analysis of their accuracy, computational cost, and real computational times. Building upon the semi-discrete formulation presented in [2,6], this work develops fully discrete forms using three explicit and three implicit methods. The performance of the proposed approaches, along with a detailed comparison between explicit and implicit solvers combined with FPM, represents the main focus of this study.

2 GOVERNING EQUATION, BOUNDARY CONDITIONS AND INITIAL CONDITION

The partial differential equation (PDE) governing transient heat conduction in anisotropic, nonhomogeneous media is given by:

$$\rho c \frac{\partial u}{\partial t} = \nabla \cdot [\mathbf{k} \nabla u] + Q, \tag{1}$$

where: $\rho(\mathbf{r})$ is density, $c(\mathbf{r})$ is a specific heat capacity, $u(\mathbf{r},t)$ is temperature field, $\mathbf{k}(\mathbf{r})$ is a thermal conductivity tensor, $Q(\mathbf{r},t)$ is a density of heat sources, ∇ is a gradient operator, $\mathbf{r}$ is a position vector, and t is time.

In order to complete the equation (1), boundary conditions have to be specified. Dirichlet and Neumann conditions are typical for heat conduction equation, and given in the following forms:

$$\begin{aligned} u &= g_{\mathrm{D}}, && \mathbf{r} \in \Gamma_{\mathrm{D}}, \\ [\mathbf{k} \nabla u] \cdot \mathbf{n} &= \mathbf{g} \cdot \mathbf{n} = g_{\mathrm{N}}, && \mathbf{r} \in \Gamma_{\mathrm{N}}, \end{aligned} \tag{2}$$

where: $\mathbf{n}$ represents the outer normal vector of the domain.

The initial condition is given as:

$$u(\mathbf{r},t)|_{t=0} = u(\mathbf{r},0). \tag{3}$$

3 SEMI-DISCRETE FORM OF THE GOVERNING EQUATION BY MESHLESS FRAGILE POINTS METHOD

In order to obtain the full-discrete form of the governing equation, it has to be noted that one approach has to be employed in order to deal with the discretisation in the space domain, while some other ODE solver has to be introduces in order to deal with the discretisation in the time domain. One of the latest approaches used for the discretisation of the heat conduction equation in the space domain is meshless Fragile Points Method (FPM). Its potential for solving those kind of problems was firstly explored through papers [2,3], while further researches and analyses given in [5] confirmed its superiority for this kind of problem in comparison to any other numerical approach known so far. That is why the FPM, specifically the FPM-Primal, was also chosen as the starting point of this study to derive the semi-discrete form of the Eq. (1).

Trial and test functions are required to support the semi-discrete form. Although different choices are possible, in this research the test functions are chosen to be identical to the trial functions. This approach ensures the symmetry of the matrices.

One of the main advantages of the Fragile Points Method (FPM) is the ability to employ piecewise polynomial functions as trial functions, with the key benefit being the ease and accuracy of numerical integration using simple Gaussian quadratures. In this study, as low as first-order polynomial is used, providing improved computational efficiency while maintaining accurate results.

To define the trial functions, the domain must be divided into a number of non-overlapping polygons (subdomains) that together cover the entire domain, with exactly one discretization point located within each subdomain (*Fig. 1*).

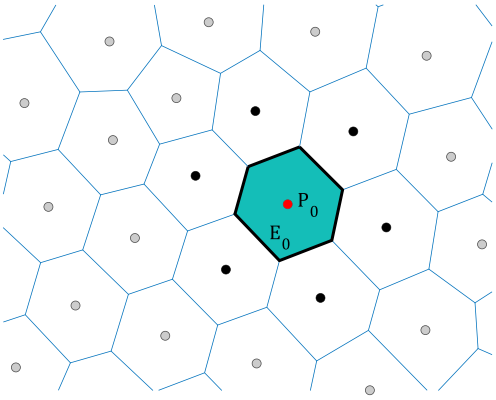

Figure 1 – Domain partitioning into subdomains in FPM

Each subdomain has its own shape function, defined such that the trial function at any point within the subdomain depends on its position vector, the function value at a specific subdomain point (point P_0 for subdomain E_0 in Fig. 1), and the gradient of the function at that specific point (P_0). On the other side, the gradient of the function at the specific point (P_0) depends on the function values at the surrounding (neighbouring) points (for P_0, these are the black points in Fig. 1). All that make the FPM truly meshless.

Process of forming of semi-discrete form of the general heat conduction equation on the basis of FPM is explained in details in [2,6]. Following on [6], final form of the general heat conduction equation has the following shape:

$$\begin{aligned}\sum_{E\in\Omega}\int_{E}\rho c v\frac{\partial u_h}{\partial t}\mathrm{d}\Omega+\sum_{E\in\Omega}\int_{E}(\mathbf{k}\nabla u_h)\cdot\nabla v\mathrm{d}\Omega-\sum_{e\in\Gamma_h}\int_{e}(\mathbf{k}[\![u_h]\!])\cdot\{\nabla v\}\mathrm{d}\Gamma-\sum_{e\in\Gamma_D}\int_{e}\{u_h\}[\![\mathbf{k}\nabla v]\!]\mathrm{d}\Gamma\\ -\sum_{e\in\Gamma_h}\int_{e}\left(\mathbf{k}\left(\{\nabla u_h\}-\frac{\eta_h}{h_e}[\![u_h]\!]\right)\right)\cdot[\![v]\!]\mathrm{d}\Gamma-\sum_{e\in\Gamma_D}\int_{e}\left[\!\!\left[\mathbf{k}\left(\nabla u_h-\frac{\eta_D}{h_e}u_h\mathbf{n}\right)\right]\!\!\right]\{v\}\mathrm{d}\Gamma\\ =\sum_{E\in\Omega}\int_{E}Qv\mathrm{d}\Omega+\sum_{e\in\Gamma_D}\int_{e}\left(\left[\!\!\left[\mathbf{k}\left(\frac{\eta_D}{h_e}g_D\mathbf{n}\right)\right]\!\!\right]\{v\}-\{g_D\}[\![\mathbf{k}\nabla v]\!]\right)\mathrm{d}\Gamma+\sum_{e\in\Gamma_N}\int_{e}g_N v\mathrm{d}\Gamma,\end{aligned}\tag{4}$$

where: u_h is the trial function, v is the test function, $[\![\ ]\!]$ and $\{\ \}$ denote the jump and average operators, respectively, η_h and η_D are the penalty parameters on internal and Dirichlet boundaries, respectively, and h_e is edge-size parameter ([1,2,7]).

Following [1,2], the trial function can be expressed in the following form:

$$u_h(\mathbf{r})=\mathbf{N}\mathbf{u},\qquad \mathbf{r}\in E_0,\tag{5}$$

while its gradient at P_0 point takes the following shape:

$$\nabla u|_{P_0}=\mathbf{B}\mathbf{u},\tag{6}$$

where:

$$\mathbf{N}=(\mathbf{r}-\mathbf{r}_0)^{\mathrm{T}}\mathbf{B}+[1\quad 0\quad\cdots\quad 0]_{1\times(m+1)},$$

$$\mathbf{B}=\left(\mathbf{A}^{\mathrm{T}}\mathbf{A}\right)^{-1}\mathbf{A}^{\mathrm{T}}\begin{bmatrix}-1&1&0&\cdots&0\\-1&0&1&\cdots&0\\\vdots&\vdots&\vdots&\ddots&\vdots\\-1&0&0&\cdots&1\end{bmatrix}_{m\times(m+1)},$$

$$\mathbf{A}=[\mathbf{r}_1-\mathbf{r}_0\quad\mathbf{r}_2-\mathbf{r}_0\quad\cdots\quad\mathbf{r}_m-\mathbf{r}_0]^{\mathrm{T}},$$

$$\mathbf{u}=[u_0\quad u_1\quad\cdots\quad u_m]^{\mathrm{T}}.$$

By introducing the heat conduction and stiffness matrices, Eq. (4) can be rewritten in a compact form:

$$\begin{aligned}\sum\mathbf{C}_E\dot{\mathbf{u}}+\sum(\mathbf{K}_E+\mathbf{K}_h+\mathbf{K}_D)\mathbf{u}\\=\sum(\mathbf{F}_E+\mathbf{F}_D+\mathbf{F}_N),\end{aligned}\tag{7}$$

or more simply:

$$\mathbf{C}\dot{\mathbf{u}}+\mathbf{K}\mathbf{u}=\mathbf{F},\tag{8}$$

where: $\mathbf{C}$ represents the global heat capacity matrix, $\mathbf{K}$ is the global thermal conductivity matrix, $\mathbf{u}$ is the vector of nodal temperatures, $\dot{\mathbf{u}}$ is a time derivative vector of the nodal temperatures, and $\mathbf{F}$ is the heat flux vector. $\mathbf{C}$ and $\mathbf{K}$ are constant, while the vector $\mathbf{F}$ can generally vary, depending on the heat sources and boundary conditions.

After introducing the trial and test functions, given by Eq. (5), into the semi-discrete form of the governing Eq. (1), expressed by Eq. (4), the individual terms of the Eq. (7) can be obtained at

the subdomain level in a way that is presented in details in [2,6].

The convergence and stability of the FPM for solving the general heat conduction equation have been demonstrated in previous studies (see [3,5,6]).

4 FULL-DISCRETE FORMS OF THE GOVERNING EQUATION BY MESHLESS FRAGILE POINTS METHOD AND VARIOUS ODE SOLVERS

To complete the numerical solution, i.e., to obtain the fully discrete form of the heat conduction equation in anisotropic, non-homogeneous media, ODE (8) must be solved. A variety of approaches can be used. One such method is the Local Variational Iteration Method (LVIM), developed in [8], which has been shown to be highly compatible with FPM in [3,5].

For this research, however, three explicit and three implicit solvers were considered, namely:

- Forward Euler (FE),
- Runge-Kutta 4th order (RK4),
- Adams-Bashforth 3th order (AB3),
- Backward Euler (BE),
- Trapezoidal Rule (TR) and
- Adams-Moulton 3th order (AM3).

Based on the concept of these six methods in combination with ODE (8), the fully discrete forms of the governing equation are summarized in *Table 1*.

Table 1 – The full-discrete forms of the governing equation obtained using FPM and six ODE solvers

Explicit	FPM + Forward Euler (FE)	$\mathbf{u}_{m+1} = \mathbf{u}_m + \Delta t \mathbf{G}_m$
	FPM + Runge-Kutta 4th order (RK4)	$\mathbf{u}_{m+1} = \mathbf{u}_m + \frac{\Delta t}{6}\mathbf{C}^{-1}(\mathbf{k}_1 + 2\mathbf{k}_2 + 2\mathbf{k}_3 + \mathbf{k}_4)$ $\mathbf{k}_1 = \mathbf{F}_m - \mathbf{K}\mathbf{u}_m$ $\mathbf{k}_2 = \mathbf{F}_{m+0.5\Delta t} - \mathbf{K}(\mathbf{u}_m + 0.5\Delta t \mathbf{k}_1)$ $\mathbf{k}_3 = \mathbf{F}_{m+0.5\Delta t} - \mathbf{K}(\mathbf{u}_m + 0.5\Delta t \mathbf{k}_2)$ $\mathbf{k}_4 = \mathbf{F}_{m+\Delta t} - \mathbf{K}(\mathbf{u}_m + \Delta t \mathbf{k}_3)$
	FPM + Adams-Bashforth method 3th order (AB3)	$\mathbf{u}_{m+1} = \mathbf{u}_m + \Delta t \mathbf{G}_m$ $\mathbf{u}_{m+2} = \mathbf{u}_{m+1} + \frac{\Delta t}{2}(3\mathbf{G}_{m+1} - \mathbf{G}_m)$ $\mathbf{u}_{m+3} = \mathbf{u}_{m+2} + \frac{\Delta t}{12}(23\mathbf{G}_{m+2} - 16\mathbf{G}_{m+1} + 5\mathbf{G}_m)$
Implicit	FPM + Backward Euler (BE)	$\mathbf{u}_{m+1} = \mathbf{u}_m + \Delta t \mathbf{G}_{m+1}$ $\mathbf{u}_{m+1} = (\mathbf{E} + \Delta t \mathbf{C}^{-1}\mathbf{K})^{-1}(\mathbf{u}_m + \Delta t \mathbf{C}^{-1}\mathbf{F}_{m+1})$
	FPM + Trapeze Rule (TR)	$\mathbf{u}_{m+1} = \mathbf{u}_m + \frac{\Delta t}{2}(\mathbf{G}_m + \mathbf{G}_{m+1})$ $\mathbf{u}_{m+1} = \left(\mathbf{E} + \Delta t \frac{1}{2}\mathbf{C}^{-1}\mathbf{K}\right)^{-1}\left(\mathbf{u}_m + \frac{\Delta t}{2}(\mathbf{G}_m + \mathbf{C}^{-1}\mathbf{F}_{m+1})\right)$
	FPM + Adams-Moulton method 3th order (AM3)	$\mathbf{u}_{m+1} = \mathbf{u}_m + \Delta t \mathbf{G}_{m+1}$ (like BE) $\mathbf{u}_{m+2} = \mathbf{u}_{m+1} + \frac{\Delta t}{2}(\mathbf{G}_{m+1} + \mathbf{G}_{m+2})$ (like TR) $\mathbf{u}_{m+3} = \mathbf{u}_{m+2} + \frac{\Delta t}{12}(-\mathbf{G}_{m+1} + 8\mathbf{G}_{m+2} + 5\mathbf{G}_{m+3})$ $\mathbf{u}_{m+3} = \mathbf{u}_{m+2} + \frac{\Delta t}{12}\left(-\mathbf{G}_{m+1} + 8\mathbf{G}_{m+2} + 5\mathbf{C}^{-1}(\mathbf{F}_{m+3} - \mathbf{K}\mathbf{u}_{m+3})\right)$ $\mathbf{u}_{m+3} = \left(\mathbf{E} + \Delta t \frac{5}{12}\mathbf{C}^{-1}\mathbf{K}\right)^{-1}\left(\mathbf{u}_{m+2} + \frac{\Delta t}{12}(-\mathbf{G}_{m+1} + 8\mathbf{G}_{m+2} + 5\mathbf{C}^{-1}\mathbf{F}_{m+3})\right)$

Δt is a time step
$\mathbf{u}_m$ is vector of temperatures in specified nodes at t_m
$\mathbf{u}_{m+1}$ is vector of temperatures in specified nodes at $t_{m+1} = t_m + \Delta t$
$\mathbf{E}$ is a unit matrix of size $n \times n$
$\mathbf{G}_m = \mathbf{C}^{-1}(\mathbf{F}_m - \mathbf{K}\mathbf{u}_m)$

5 TIME COMPLEXITY OF THE PROPOSED ALGORITHMS

The formation of the $\mathbf{C}$ and $\mathbf{K}$ matrices is not time-consuming in FPM. By analysing the procedure used to construct them, it can be concluded that their formation can be performed with an approximate complexity of $O(n)$, where n is the number of nodes, i.e., the number of domain points. However, the inversion of the $\mathbf{C}$ matrix can be time-consuming. Using Gaussian elimination, this can be achieved with a complexity of $O(n^3)$. However, since FPM yields a positive definite, symmetric, sparse, and well-structured matrix, advanced solvers such as sparse Cholesky or multigrid methods can be applied, drastically reducing the computational cost – sometimes even approaching linear complexity with respect to n.

In all six algorithms listed in Table 1, the multiplication of an $n \times n$ matrix with a vector of length n is the most computationally intensive operation within each time step, with complexity $O(n^2)$ per step. Consequently, the overall complexity of all six approaches can be roughly estimated as $O(n_t n^2)$, where n_t is the number of time steps. This is more computationally demanding than the inversion of the $\mathbf{C}$ matrix, regardless of the number of time steps, and is therefore considered the dominant operation.

However, in practice, the six algorithms don't have identical computational costs. For example, in Euler methods, the multiplication of an $n \times n$ matrix with an $n \times 1$ matrix occurs twice per time step, while in the 4th-order Runge-Kutta method it occurs five times, so the latter is expected to be approximately 2.5 times slower.

6 NUMERICAL EXAMPLES

The capabilities of FPM are demonstrated through several numerical examples in 1D and 2D, for which analytical solutions are available in the literature. None of them involve internal heat sources. For each example, a comparison of the six ODE solvers was performed in terms of accuracy, computational time, and ability to solve the problem. Point distributions were mostly uniform, while both the number of points and the number of time steps were varied. Accuracy was estimated based on the relative error value calculated using the Lebesgue norm:

$$r_0 = \frac{\|u_h - \phi\|_{L^2}}{\|\phi\|_{L^2}}, \qquad \|\phi\|_{L^2} = \sqrt{\left(\int_\Omega \phi^2 \mathrm{d}\Omega\right)}. \quad (9)$$

Previous studies [3,6] provide an overview of the choice of penalty parameters. In these works, r_0 values were estimated through a number of examples, considering a wide range of penalty parameters values, typically from 10^{-5} to 10^5. Based on this previous experience, for all 1D problems, penalty parameters of $\eta_\mathrm{h} = 100$ and $\eta_\mathrm{D} = 500$ were used, whereas for all 2D problems, the values $\eta_\mathrm{h} = \eta_\mathrm{D} = 2$ were adopted.

Apart from the penalty parameter itself, stabilization is influenced by the dimensionality of the element boundaries. In 1D, boundary reduces to point, providing very little "contact area" for flux stabilization. Consequently, higher penalty parameters are typically required in 1D problems compared to 2D or 3D.

As for the edge size parameter h_e, a unit value was taken for 1D problems, while the boundary length was taken for 2D problems.

All codes were executed on a PC of the following specifications: Intel(R) Core(TM) i3-9100T CPU @ 3,10 GHz; RAM 8,00 GB; Intel(R) UHD Graphics 630.

The first example considers 1D transient heat conduction through a homogeneous medium with $x \in [0,1]$. The thermal diffusivity is set to 1. The initial and mixed boundary conditions are specified as follows: $u(x;0) = 1, \nabla u(0;t) = 0, u(1;t) = 0$.

The analytical solution is provided in [9].

Fig. 2 illustrates the comparison between the analytical solution and the numerical solution obtained using FPM in combination with the Backward Euler scheme for the first problem at several time points, with 50 uniformly distributed domain nodes and a time step of 10^{-4}. Table 2 presents the values of r_0 error averaged per time step within the interval $t \in [0,1]$.

As can be seen from *Fig. 2*, this problem is stiff. Consequently, explicit methods struggle to produce accurate results unless a very large number of time steps is used relative to the number of nodes. In contrast, implicit methods can provide highly accurate results even with a small number of time steps, although accuracy improves further as the number of time steps increases. Table 2 also confirms that the computational times for the FE and BE methods are roughly the same and lower than that of the RK4 method.

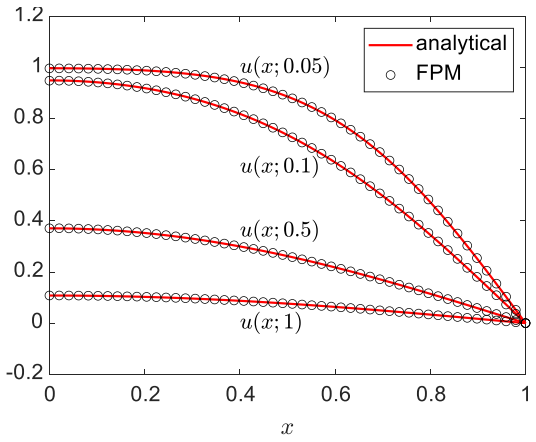

Figure 2 – Comparison of analytical and FPM solutions for the first example

Table 2 – The average values of r_0 error and computational times for the first example

n		10			100		
n_t		10^3	10^4	10^5	10^3	10^4	10^5
FE	r_0	-	$3.0\cdot10^{-2}$	$3.0\cdot10^{-2}$	-	-	$3.2\cdot10^{-4}$
	CT	-	0.11	0.47	-	-	3.63
RK4	r_0	-	$3.0\cdot10^{-2}$	$3.0\cdot10^{-2}$	-	-	$3.2\cdot10^{-4}$
	CT	-	0.13	0.67	-	-	4.26
AB3	r_0	-	-	$3.0\cdot10^{-2}$	-	-	-
	CT	-	-	0.45	-	-	-
BE	r_0	$3.1\cdot10^{-2}$	$3.0\cdot10^{-2}$	$3.0\cdot10^{-2}$	$2.2\cdot10^{-3}$	$5.2\cdot10^{-4}$	$3.6\cdot10^{-4}$
	CT	0.06	0.09	0.41	0.09	0.47	3.48
TR	r_0	$3.1\cdot10^{-2}$	$3.0\cdot10^{-2}$	$3.0\cdot10^{-2}$	$4.4\cdot10^{-3}$	$3.6\cdot10^{-4}$	$3.4\cdot10^{-4}$
	CT	0.07	0.10	0.41	0.08	0.43	3.28
AM3	r_0	-	$3.0\cdot10^{-2}$	$3.0\cdot10^{-2}$	-	-	$3.4\cdot10^{-4}$
	CT	-	0.11	0.44	-	-	3.95
CT is computational time in seconds							

In the second 1D problem, transient heat conduction through a homogeneous media in the domain $x \in [0,1]$ is analysed. The thermal diffusivity is set to 1. In this case, both boundaries are adiabatic (zero-Neumann boundary condition). The initial condition is specified as follows:

$$u(x;0) = \begin{cases} 0, & 0 \le x \le \frac{1}{2} \\ 2x, & \frac{1}{2} < x \le 1 \end{cases}.$$

The analytical solution is provided in [10].

Fig. 3 shows the comparison between the analytical solution and the numerical solution obtained using FPM in combination with the Euler Forward scheme for the second problem at several time points, with 50 uniformly distributed domain nodes and a time step of 10^{-4}. Table 3 presents the values of r_0 error averaged per time step within the interval $t \in [0,1]$.

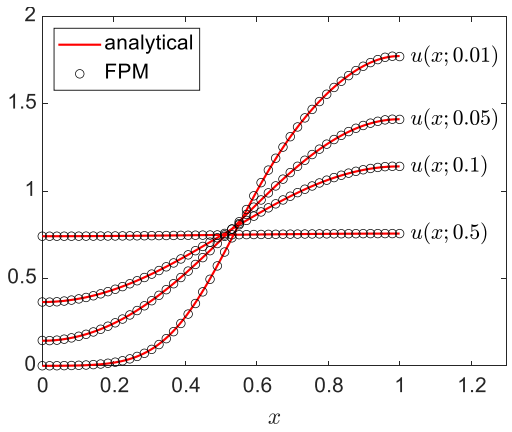

Figure 3 – Comparison of analytical and FPM solutions for the second example

Table 3 – The average values of r_0 error and computational times for the second example

n		10			100		
n_t		10^3	10^4	10^5	10^3	10^4	10^5
FE	r_0	-	$6.0\cdot10^{-3}$	$6.0\cdot10^{-3}$	-	-	$1.0\cdot10^{-4}$
	CT	-	0.17	0.36	-	-	2.43

RK4	r_0	-	$6.0\cdot10^{-3}$	$6.0\cdot10^{-3}$	-	-	$1.0\cdot10^{-4}$
	CT	-	0.16	0.55	-	-	2.97
AB3	r_0	-	$6.0\cdot10^{-3}$	$6.0\cdot10^{-3}$	-	-	$1.1\cdot10^{-4}$
	CT	-	0.12	0.30	-	-	1.30
BE	r_0	$6.4\cdot10^{-3}$	$6.0\cdot10^{-3}$	$6.0\cdot10^{-3}$	$6.8\cdot10^{-4}$	$1.7\cdot10^{-4}$	$1.2\cdot10^{-4}$
	CT	0.06	0.11	0.29	0.10	0.31	2.24
TR	r_0	$6.0\cdot10^{-3}$	$6.0\cdot10^{-3}$	$6.0\cdot10^{-3}$	$3.0\cdot10^{-4}$	$1.1\cdot10^{-4}$	$1.1\cdot10^{-4}$
	CT	0.07	0.12	0.32	0.10	0.23	1.57
AM3	r_0	$6.0\cdot10^{-3}$	$6.0\cdot10^{-3}$	$6.0\cdot10^{-3}$	-	$1.1\cdot10^{-4}$	$1.1\cdot10^{-4}$
	CT	0.07	0.12	0.34	-	0.35	2.72
CT is computational time in seconds							

As can be seen from both *Figure 3* and *Table 3*, very precise results are obtained, with the average relative error around 0.6%, even with a very small number of domain points and time steps. However, significantly better results can be achieved by increasing the number of domain points and time steps, while still incurring very low computational costs on a PC with modest performance. Again, explicit methods struggle to produce accurate results unless the number of time steps is very high relative to the number of domain points.

In the third problem, transient 1D heat conduction through a non-homogeneous media is analysed. Its characteristics are given as follows:

$$y \in [0,1], \qquad \rho(y) = 1,$$
$$c(y) = \exp(3y), \quad k(y) = \exp(3y).$$

Initial and Dirichlet boundary conditions are given as:

$$u(y;0) = 1, \quad u(0;t) = 1, \quad u(L;t) = 20.$$

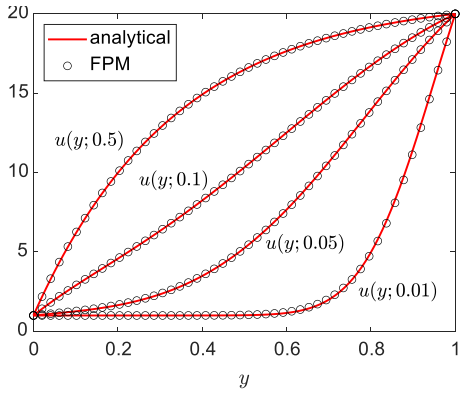

Figure 4 – Comparison of analytical and FPM solutions for the third example

Analytical solution is given in [11], while the FPM results are presented in *Fig. 4* and *Table 4*.

Table 4 – The average values of r_0 error and computational times for the third example

n		10			100		
n_t		10^3	10^4	10^5	10^3	10^4	10^5
FE	r_0	-	$1.5\cdot10^{-2}$	$1.5\cdot10^{-2}$	-	-	$3.6\cdot10^{-4}$
	CT	-	0.44	2.69	-	-	15.10
RK4	r_0	-	$1.5\cdot10^{-2}$	$1.5\cdot10^{-2}$	-	-	$3.6\cdot10^{-4}$
	CT	-	0.62	5.06	-	-	18.46
AB3	r_0	-	-	$1.5\cdot10^{-2}$	-	-	-
	CT	-	-	2.37	-	-	-
BE	r_0	$1.5\cdot10^{-2}$	$1.5\cdot10^{-2}$	$1.5\cdot10^{-2}$	$1.5\cdot10^{-3}$	$4.9\cdot10^{-4}$	$3.8\cdot10^{-4}$
	CT	0.11	0.29	2.35	0.13	1.05	14.88
TR	r_0	$1.7\cdot10^{-2}$	$1.5\cdot10^{-2}$	$1.5\cdot10^{-2}$	$9.8\cdot10^{-3}$	$4.9\cdot10^{-4}$	$3.7\cdot10^{-4}$
	CT	0.11	0.31	2.42	0.13	0.98	14.17
AM3	r_0	-	$1.5\cdot10^{-2}$	$1.5\cdot10^{-2}$	-	-	$3.7\cdot10^{-4}$
	CT	-	0.30	2.42	-	-	15.47
CT is computational time in seconds							

Figure 4 shows the comparison between the analytical solution and the numerical solution obtained using FPM in combination with the Trapeze Rule scheme for the third problem at several time points, with 50 uniformly distributed domain points and a time step of 10^{-4}, while Table 4 presents the values of r_0 error averaged per time step within the interval $t \in [0,1]$. The results indicate that highly accurate results can be obtained using this approach even with a relatively small number of domain points and time steps when implicit schemes are applied. Conversely, explicit schemes can also yield very good results, but only when a large number of time steps is used.

In the fourth example, the first in 2D, transient heat conduction across a homogeneous, isotropic domain defined by $x \in [0,1]$ and $y \in [0,1]$ is analysed. The density ρ and specific heat capacity c are both set to 1, while the thermal conductivity tensor $\mathbf{k}$ is equal to the Kronecker delta function. The analytical solution for this problem is provided in [12]. All boundaries are time-dependent Dirichlet boundaries, except $x = 1$ where a Neumann condition is imposed.

Expressions for all four boundary conditions, as well as for the initial condition (for $t_0 = 0$), are derived from the analytical solution.

Fig. 5 shows a comparison between the analytical solution, the numerical results obtained using the Method of Fundamental Solutions (MFS) presented in [12], and the numerical results obtained using FPM with the FE scheme and a time step of 10^{-4}. The results are presented along the Neumann boundary at $t = 1.5$. Numerical results were obtained using 121 uniformly distributed points. Two FPM solutions are shown in Fig. 5 – one where 40 of the 121 points are located on the boundaries, and another where no points are placed directly on the boundaries. An error of $r_0 = 0.00253$ was obtained when points were placed directly on the boundaries, while an error of $r_0 = 0.00165$ was obtained when no points were placed on the boundaries. For both point distribution approaches, the FPM results are very good. *Figure 5* also suggests that FPM provides slightly better accuracy than the MFS.

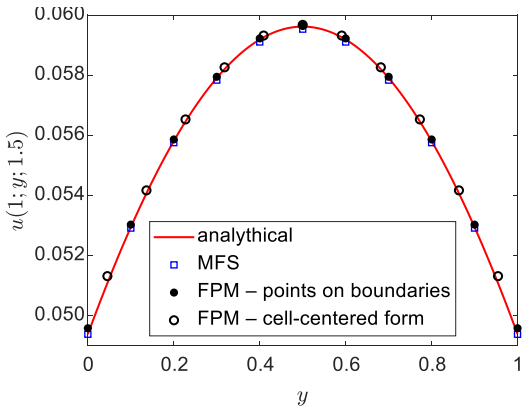

Figure 5 – Comparison of analytical MFS, and FPM solutions for the fourth example at $x = 1$ and $t = 1.5$

The same problem was solved using 144 domain points. The temperature distribution over the domain at $t = 1$ is shown in Fig. 6, where three FPM solutions are presented:

- a uniform point distribution with 44 points set directly on the boundaries,
- a random point distribution with 44 points set directly on the boundaries, and
- a uniform point distribution with no points placed directly on the boundaries.

When compared with the analytical solution (*Fig. 6a*), all three FPM configurations (*Fig. 6b*) yield very good results.

For the fourth example, Table 5 presents the values of the r_0 error at $t = 1$ for the results obtained using FPM with different ODE solvers and varying numbers of uniformly distributed points and time steps. In all cases, some points were positioned on the boundaries. The results show that accurate solutions can be achieved even with a relatively small number of domain points. However, as observed in the previous examples, implicit solvers appear to perform better, as they can produce accurate results even when the number of time steps is not significantly greater than the number of domain points. Furthermore, increasing the number of domain points and time steps reduces the relative error, confirming the convergence of the FPM.

a)

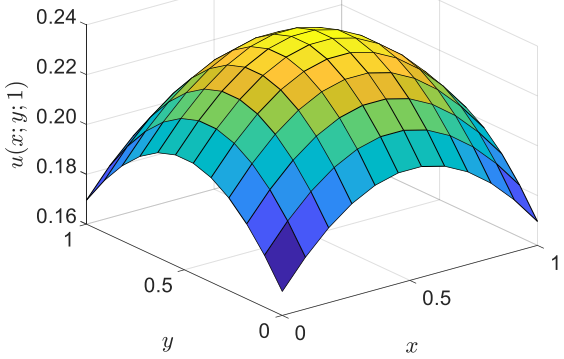

b)

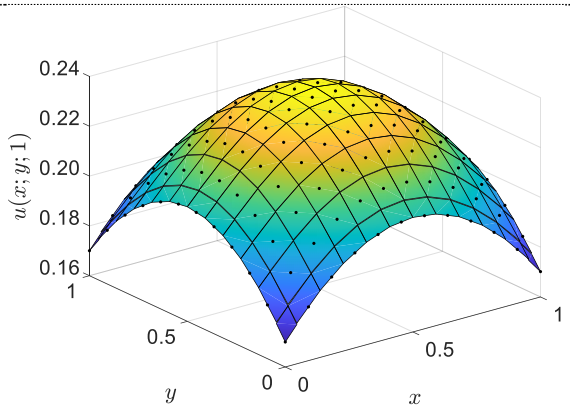

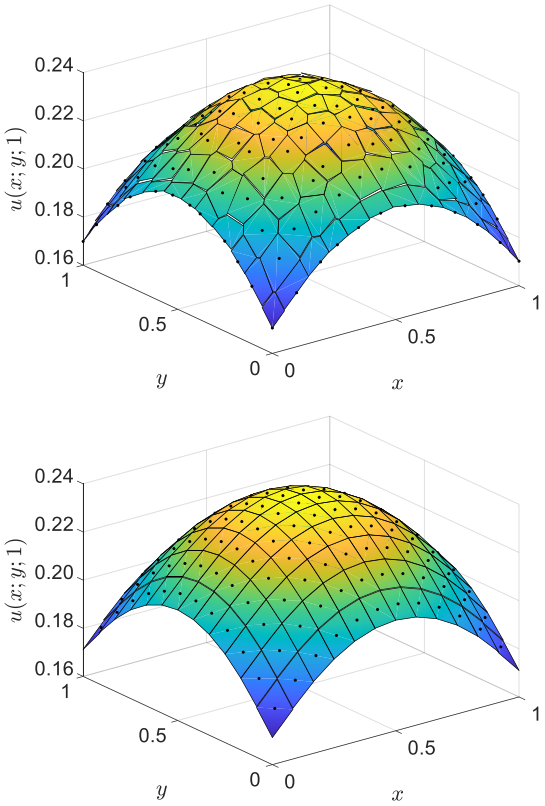

Figure 6 – Results of the fourth example at $t = 1$: a) Analytical result; b) FPM results

Table 5 – Relative error r_0 at $t = 1$ and computational times for the fourth example

n		10×10			100×100		
n_t		10^3	10^4	10^5	10^3	10^4	10^5
FE	r_0	-	$3.1\cdot10^{-3}$	$3.1\cdot10^{-3}$	-	-	$2.5\cdot10^{-4}$
	CT	-	5.00	49.29	-	-	492.77
RK4	r_0	-	$3.2\cdot10^{-3}$	$3.1\cdot10^{-3}$	-	-	$2.8\cdot10^{-4}$
	CT	-	23.78	135.37	-	-	879.53
AB3	r_0	-	$3.2\cdot10^{-3}$	$3.1\cdot10^{-3}$	-	-	$2.7\cdot10^{-4}$
	CT	-	8.66	40.65	-	-	205.03
BE	r_0	$4.1\cdot10^{-3}$	$3.2\cdot10^{-3}$	$3.1\cdot10^{-3}$	$2.4\cdot10^{-3}$	$4.3\cdot10^{-4}$	$2.7\cdot10^{-4}$
	CT	0.59	9.56	46.03	5.17	49.42	467.35
TR	r_0	$3.1\cdot10^{-3}$	$3.1\cdot10^{-3}$	$3.1\cdot10^{-3}$	$2.5\cdot10^{-4}$	$2.5\cdot10^{-4}$	$2.5\cdot10^{-4}$
	CT	0.55	7.02	40.43	3.68	35.40	334.43
AM3	r_0	$3.1\cdot10^{-3}$	$3.1\cdot10^{-3}$	$3.1\cdot10^{-3}$	-	$2.5\cdot10^{-4}$	$2.5\cdot10^{-4}$
	CT	0.57	6.83	46.53	-	60.69	585.18
CT is computational time in seconds							

In the fifth example, homogeneous and non-homogeneous isotropic and anisotropic media are analysed. The domain is square-shaped with a side length of L. The initial and Dirichlet boundary conditions are defined as follows:

$$u(x;y;0) = u(x;0;t) = 1, \quad u(x;L;t) = 20.$$

A symmetric boundary condition is imposed on the remaining boundaries (see [2]).

The media characteristics are as follows:

$$\rho(x;y) = 1, \quad c(x;y) = \exp(2\delta y/L),$$

$$\mathbf{k}(x;y) = \exp(2\delta y/L)\begin{bmatrix}\hat{k}_{11} & \hat{k}_{12}\\ \hat{k}_{21} & \hat{k}_{22}\end{bmatrix},$$

where for the isotropic media $\hat{k}_{ij} = \delta_{ij}$, for the anisotropic $\hat{k}_{11} = \hat{k}_{22} = 2$, $\hat{k}_{12} = \hat{k}_{21} = 1$, for the homogenous media $\delta = 0$, and for the non-homogenous media $\delta = 1.5$.

Analytical solution is given in [13].

The comparison between the analytical solution and the FPM combined with the BE scheme is presented in Figure 7. The results are demonstrated for $x = L/2$, but they are identical across any parallel plane. The problem was solved using a 15×15 grid over the $t \in [0,1]$ with a time step of 10^{-4}.

a)

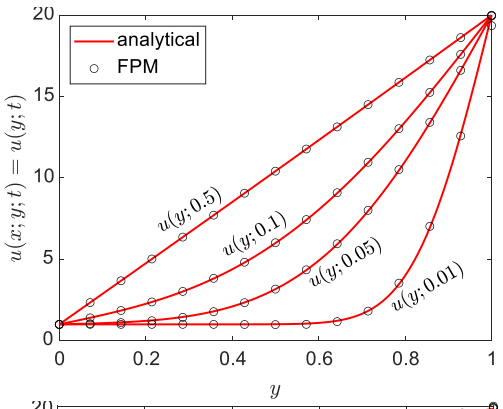

b)

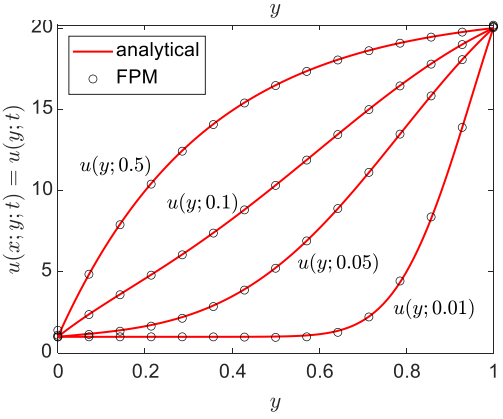

c)

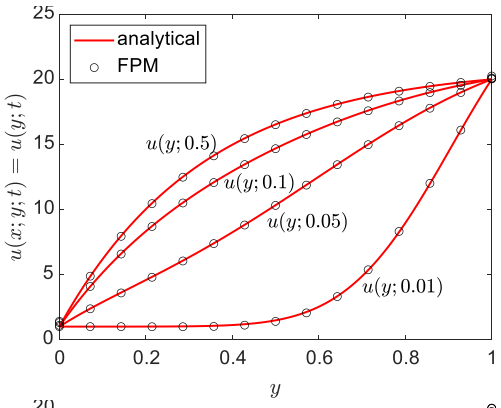

d)

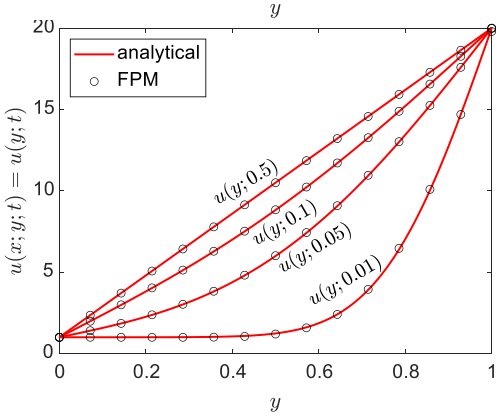

Figure 7 – Analytic and FPM results of the fifth example: a) homogenous isotropic media; b) non-homogenous isotropic media; c) non-homogenous anisotropic media; d) homogenous anisotropic media

7 CONCLUSIONS

Through various 1D and 2D examples, the suitability of the FPM for solving general heat conduction problems has been confirmed. The FPM demonstrates strong compatibility with different ODE solvers. Its significant advantages include the symmetry and sparsity of the resulting matrices, as well as the linearity of the trial and test functions. All these features contribute to the computational efficiency of the method, as evidenced by very low computational times, even with a large number of domain points and time steps, on a low-performance computer used in this study.

All six algorithms developed in this research can be executed with an approximate computational complexity of $O(n_t n^2)$. For the specific problems analysed in this paper, it was shown that implicit methods can perform as efficiently as the simple Forward Euler method while maintaining the same level of accuracy. Moreover, for stiff problems, explicit methods fail to produce satisfactory results unless the number of time steps is significantly greater than the number of domain points, whereas implicit methods provide accurate results even with a relatively small number of time steps.

The presence of non-homogeneity and anisotropy does not introduce difficulties for FPM. Although none of the problems in this paper involve heat sources, their presence would not pose any complications either – the first term on the right-hand side of Eq. (4) would simply become non-zero and could be evaluated straightforwardly using Gaussian quadratures.

8 REFERENCES

[1] Dong, L., Yang, T., Wang, K., & Atluri, S. N. (2019). A new fragile points method (FPM) in computational mechanics, based on the concepts of point stiffnesses and numerical flux corrections. *Engineering Analysis with Boundary Elements, 107*, 124–133. https://doi.org/10.1016/j.enganabound.2019.07.009

[2] Guan, Y., Grujicic, R., Wang, X., Dong, L., & Atluri, S. N. (2020). A new meshless "fragile points method" and a local variational iteration method for general transient heat conduction in anisotropic nonhomogeneous media. Part I: Theory and implementation. *Numerical Heat Transfer, Part B: Fundamentals, 78*(2), 71–85. https://doi.org/10.1080/10407790.2020.1747278

[3] Guan, Y., Grujicic, R., Wang, X., Dong, L., & Atluri, S. N. (2020). A new meshless "fragile points method" and a local variational iteration method for general transient heat conduction in anisotropic nonhomogeneous media. Part II: Validation and discussion. *Numerical Heat Transfer, Part B: Fundamentals, 78*(2), 86–109. https://doi.org/10.1080/10407790.2020.1747283

[4] Guan, Y., Grujičić, R., Wang, X., Dong, L., & Atluri, S. N. (2020, November 16–19). *A new and efficient meshless computational approach for transient heat conduction in anisotropic nonhomogeneous media: Fragile points method and local variational iteration scheme.* In *Proceedings of the ASME 2020 International Mechanical Engineering Congress and Exposition (IMECE2020)*, Portland, OR, USA.

[5] Subani, N., Jamaluddin, F., Mohamed, M. A. H., & Badrolhisam, A. D. H. (2020). Analytical solution of homogeneous one-dimensional heat equation with Neumann boundary conditions. *Journal of Physics: Conference Series, 1551,* 012002. https://doi.org/10.1088/1742-6596/1551/1/012002

[6] Guan, Y., & Atluri, S. N. (2021). Meshless fragile points methods based on Petrov–Galerkin weak-forms for transient heat conduction problems in complex anisotropic nonhomogeneous media. *International Journal for Numerical Methods in Engineering, 122*(16), 4055–4092. https://doi.org/10.1002/nme.6692

[7] Grujičić, R. (2023). *Meshless fragile points method (FPM) for fluid flow around aerodynamic shapes and heat distribution problems* [Doctoral dissertation, University of Belgrade, Faculty of Mechanical Engineering].

[8] Arnold, D. N., Brezzi, F., Cockburn, B., & Marini, L. D. (2002). Unified analysis of discontinuous Galerkin methods for elliptic problems. *SIAM Journal on Numerical Analysis, 39*, 1749–1779. https://doi.org/10.1137/S0036142901384162

[9] Wang, X. (2019). *Optimized Picard iteration methods for nonlinear dynamical systems with non-smooth nonlinearities, and orbital mechanics* [Doctoral dissertation, Texas Tech University].

[10] Mackowski, D. W. (2011). *Conduction heat transfer: Notes for MECH 7210*. Auburn, AL: Mechanical Engineering Department, Auburn University.

[11] Sladek, V., Sladek, J., Tanaka, M., & Zhang, C. (2005). Transient heat conduction in anisotropic and functionally graded media by local integral equations. *Engineering Analysis with Boundary Elements, 29*, 1047–1065. https://doi.org/10.1016/j.enganabound.2005.05.011

[12] Johansson, B. T., Lesnic, D., & Reeve, T. (2011). A method of fundamental solutions for two-dimensional heat conduction. *International Journal of Computer Mathematics, 88*(8), 1697–1713. https://doi.org/10.1080/00207160.2010.522233

[13] Gambaruto, A. M. (2015). Computational haemodynamics of small vessels using the moving particle semi-implicit (MPS) method. *Journal of Computational Physics, 302,* 68–96. https://doi.org/10.1016/j.jcp.2015.08.039